INSTITUTE OF PHYSICS PUBLISHING METROLOGIA
Metrologia **43** (2006) 383–388 doi:10.1088/0026-1394/43/5/007

An upper bound to the frequency dependence of the cryogenic vacuum-gap capacitor

Neil M Zimmerman, Brian J Simonds and Yicheng Wang

National Institute of Standards and Technology[1], Gaithersburg, MD 20899, USA

E-mail: neilz@mailaps.org

Received 11 April 2006, accepted for publication 23 May 2006
Published 6 September 2006
Online at stacks.iop.org/Met/43/383

Abstract
In attempting to develop a capacitance standard based on the charge of the electron, one question which has been open for many years is the frequency dependence of the vacuum-gap cryogenic capacitor; the crucial difficulty has been: How do we measure frequency dependence down to 0.01 Hz? In this paper, we succeed in putting an upper bound on the frequency dependence, from 0.01 Hz to 1 kHz, of about 2×10^{-7}. We do this by considering a model for the dispersion in the surface insulating films on the surface of the Cu electrodes; the crucial prediction of this model is that the dispersion falls to very low values at low temperatures. By measuring the frequency dependence over a restricted range of frequencies, we have verified this prediction, and thus provide adequate support to conclude that the model is correct. We also point out that, independent of the capacitance standard, this cryogenic capacitor provides a frequency-independent standard for measurements in fields such as the low-temperature dynamics of amorphous materials.

1. Motivation

The electron-counting capacitance standard (ECCS) aims to provide a standard of capacitance based on the charge of the electron [1,2]. The basic mode of operation of the standard [3] is as follows: in the 'pumping' phase, we will use a single-electron tunnelling pump based on the Coulomb blockade [4] to pump a counted number of electrons (about 10 million) onto the plate of a cryogenic vacuum-gap capacitor. By measuring the voltage that develops, we can determine the value of the capacitor by $C = Q/V = Ne/V$, where e and N are the charge of the electron and the number of electrons pumped, respectively. In the second 'comparison' phase, we will connect the cryogenic capacitor to a room-temperature system (either a standard capacitor or a capacitance bridge) and thus calibrate the room-temperature standard. We have been working on developing the ECCS for a number of years, and have overcome quite a few technical challenges. However, there has been one open question which, until now, we have not been able to address. This question concerns the frequency dependence of the vacuum-gap capacitor: in the pumping phase of the ECCS, the voltage across the capacitor will follow a periodic but non-sinusoidal signal at about 0.01 Hz; in the comparison phase, the voltage across the capacitor will follow a sinusoidal signal at 1 kHz.

Since our goal is to develop the ECCS with a total uncertainty of about $\Delta C/C \approx 10^{-7}$, this means that we must assess the frequency dependence of our vacuum-gap capacitor over the frequency range from 0.01 Hz to 1 kHz, with an uncertainty no greater than 10^{-7}. This is a daunting task.

Experimentally, such a determination appears to be impossible to achieve, and in fact impossible to even approach. While there have been a number of determinations of frequency-dependent capacitance, they have all been in the audio-frequency range. As an example, a frequency-dependent measurement which has perhaps the best combination of uncertainty and frequency dependence [5] demonstrated a measurement from 50 Hz to 20 kHz, with a relative uncertainty as large as 0.6×10^{-6}; the uncertainty

[1] Quantum Electrical Metrology Division, Electronics and Electrical Engineering Laboratory, Technology Administration, US Department of Commerce. http://www.setg.nist.gov. Official contribution of the National Institute of Standards and Technology, not subject to copyright in the United States.

reduced substantially at higher frequencies. This last point illustrates a general feature: the uncertainty of frequency-dependent capacitance measurements gets larger and larger as the frequency decreases; in part, this is due to the increasing type A uncertainty in the null detector used in such capacitor comparisons.

Obviously, the best frequency-dependent capacitance measurement to date will not suffice for our goal. In addition, as we try to increase the frequency range another four decades (from 50 Hz down to 0.01 Hz), it is evident that the experimental uncertainty will rise a great deal more. Thus, if we have any hope of using the ECCS, we must develop another route for determining the frequency dependence of the cryogenic capacitor C_{cryo}.

Since we have no hope of experimentally determining the frequency dependence of C_{cryo}, we have chosen instead to develop a model which allows us to put an upper bound on the frequency dependence. The crucial observation of this model is that the effect of the imperfections in the surface insulating films which would lead to a frequency dependence decreases rapidly with temperature; thus, since we will operate the vacuum-gap capacitor at very low temperatures, we can demonstrate that C_{cryo} has negligibly small frequency dependence at the temperatures at which we operate. We will develop this model in the following section.

Because this is a new model, we have also done measurements over a limited range of frequencies similar to that referenced above [5]; these measurements show very clearly that the frequency dependence of C_{cryo} falls rapidly with temperature. These measurements provide adequate support to the model, so that we may then use the model to assign a maximum frequency dependence for C_{cryo} over the entire frequency range of interest in the ECCS.

2. Introduction

There has been a fair amount of previous work on the frequency dependence of capacitors [5–10] for standards applications. In general, the frequency dependence arises from two sources: (1) At higher frequencies (typically above about 1 kHz), the apparent capacitance increases with frequency, $\Delta C(f) \propto \omega^2$. This frequency dependence is well understood: the combination of in-line inductances and stray capacitances leads to this effect; the effect is commonly known as 'cable loading'. Because this effect is well understood, the size of the apparent frequency dependence arising from this effect can be accurately calculated, and it is a standard procedure to correct $C(f)$ for this effect. Since the correction for the offset due to this effect is a standard procedure, and because the size of the effect is small below 1 kHz, we will not consider it further. Instead, we will concentrate in this paper on the other source of frequency dependence. (2) At lower frequencies, dielectric dispersion and dissipation in the surface insulating films covering the metal electrodes of a vacuum-gap capacitor dominate the frequency dependence [11].

We have previously attempted to measure the time dependence of C_{cryo} for two reasons: (1) Since we require that the leakage through C_{cryo} be very small [12], the leakage resistance value must be greater than about $10^{21}\,\Omega$. One way to measure the leakage resistance value is to put a step voltage onto one plate of the cryogenic capacitor, and measure the charge flow off of the other plate of the capacitor. In a previous measurement [13] we demonstrated the requisite high resistance value. (2) In addition, it is also possible to determine an effective frequency dependence of capacitance from this same measurement. In this work [13], we were able to put an upper bound on the relative frequency dependence of C_{cryo} of about 10^{-6} from 2 Hz to 10 Hz; these frequency limits were set by experimental considerations and could be increased somewhat in the future.

3. Model

3.1. General considerations

In any insulator, we can define the frequency-dependent dielectric function as

$$\epsilon_1 \equiv \epsilon + \delta\epsilon(f) - \mathrm{i}\epsilon'',$$

Here, ϵ is a constant, the second term is the dispersion (frequency dependence of the real part of ϵ_1) and the third term is the dissipation or loss (imaginary part of ϵ_1). For a perfect insulator, there is no dispersion and no loss; these terms arise from the imperfections in the lattice as dipoles respond to an applied electric field by absorbing energy from the field.

We will be concerned with the dispersion in insulating films formed on the surface of the metal electrodes that make up the vacuum-gap capacitor. These insulating films are not deliberately introduced in the assembly of the capacitor; instead, they arise due to unwanted contamination or oxidation of the metal electrodes in ambient conditions. Because of this, it is likely that the surface films are highly defected and thus exhibit a substantial amount of dispersion.

3.2. Model

Consider an ideal, infinite (no fringing fields) parallel-plate capacitor filled with two dielectrics, of thicknesses d_1 and d_2, and dielectric functions ϵ_1 and ϵ_2. From simple electrostatics, it is easy to show that the total capacitance is

$$C = \frac{\epsilon_0 A}{d_1/\epsilon_1 + d_2/\epsilon_2},$$

where ϵ_0 and A are the electric constant and the capacitor area, respectively; ϵ_1 and ϵ_2 are unitless. In the case where $d_1/\epsilon_1 \ll d_2/\epsilon_2$ (d_1 is the thin film, d_2 is vacuum, so $\epsilon_2 = 1$), the total capacitance is

$$C \approx \frac{\epsilon_0 A}{d_2}[1 - d_1/d_2\epsilon_1].$$

If we assume that the non-idealities are small,

$$\delta\epsilon(f), \quad \epsilon'' \ll \epsilon,$$

then we can obtain

$$\frac{1}{\epsilon_1} \approx \frac{1}{\epsilon}\,[1 - \delta\epsilon(f)/\epsilon + \mathrm{i}\epsilon''/\epsilon].$$

Finally,

$$C \approx \frac{\epsilon_0 A}{d_2}\left[\left(1 - \frac{d_1}{d_2\epsilon}\right) + \frac{d_1}{d_2}\frac{1}{\epsilon}\frac{\delta\epsilon(f)}{\epsilon} - \mathrm{i}\frac{d_1}{d_2}\frac{1}{\epsilon}\frac{\epsilon''}{\epsilon}\right]. \quad (1)$$

Now, how do we interpret these non-ideal, possibly frequency-dependent terms? If we look at a non-ideal capacitor as a combination of a frequency-dependent ideal capacitor $C_0 + \Delta C(f)$ and an ideal resistor R in parallel, then the total frequency-dependent non-ideal capacitance is

$$C = C_0(1 + \Delta C(f)/C_0) + 1/\mathrm{i}\omega R. \tag{2}$$

The frequency dependence comes from the frequency dependence of the real part of C. Identifying this with the corresponding term of equation (1), we see that the apparent frequency dependence of C arises as

$$\frac{\Delta C(f)}{C} \approx \left(\frac{d_1}{d_2}\right)\left(\frac{1}{\epsilon}\right)\left(\frac{\delta\epsilon(f)}{\epsilon}\right), \tag{3}$$

It is clear that what we want is for this to be small.

The dispersion and the loss are related to each other through the Kramers–Kronig relations; in fact, they must be of approximately the same size. A standard result, for an imaginary part of the dielectric function $\epsilon''(\omega) < x$ (x a constant) for $\omega_1 < \omega < \omega_2$, and zero elsewhere, is that the real part of the dielectric function (in the same frequency range) obeys

$$\delta\epsilon(f) \leqslant \frac{x}{\pi} \ln \frac{\omega_2^2 - \omega^2}{\omega^2 - \omega_1^2}, \tag{4}$$

and smaller elsewhere. This relationship will help us later in calculating the total $\Delta C(f)$.

3.3. Identity and thickness of surface films

The material used in our vacuum-gap capacitor is oxygen-free high conductivity (OFHC) Cu. The native oxide is Cu_2O, as determined from XPS [14]; the growth of this air-formed oxide is self-limiting, with a thickness of about 3 nm [14].

We have performed a surface analysis on the plates of our vacuum-gap capacitor:

1. Clean plates with organic solvents.
2. Measure identity of elements on surface using Auger analysis.
3. Remove a small portion of the surface contamination and/or Cu (typically, a few nanometres) by sputtering with high-energy ions.
4. Repeat Auger analysis.

We would repeat this process for a specific spot on the surface of the plate until the Auger analysis showed only Cu. This process allowed us to identify the elements on the surface; by measuring the total amount of sputtering time necessary to remove everything except the Cu, we could measure the total thickness of the surface film. An example of the Auger spectra before and after sputter-cleaning is shown in figure 1. Typically, we required etching times between 2 min and 4 min to remove all of the surface film; the average time was about 2.5 min.

The Auger analysis shows that the surfaces of our Cu plates are not heavily contaminated, and thus probably have a typical native oxide (thickness 3 nm). As a calibration of the sputter analysis, 5 min of sputter-etching removed 15 nm of SiO_2. Based on a comparative study of ion sputtering of oxides of Si and Cu [15], our measured average sputtering time of 2.5 min would correspond to an average Cu_2O thickness of 11 nm. In order to form a conservative estimate, we choose the larger of these two (3 nm versus 11 nm), and thus conclude that the thickness of the surface film is 10 nm.

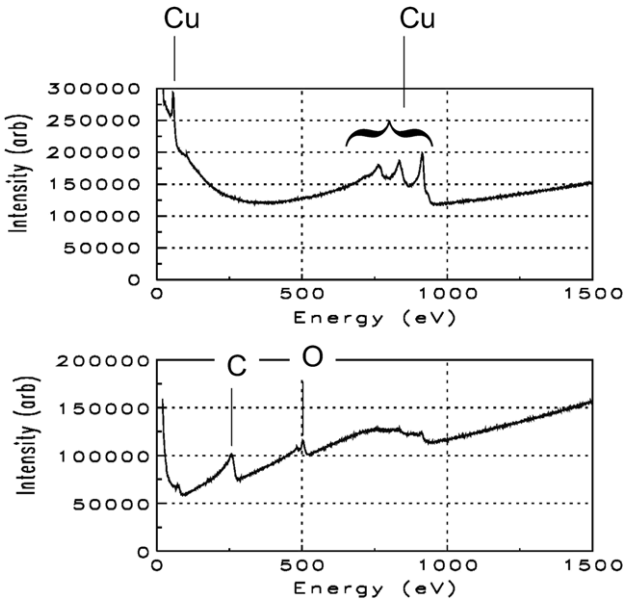

Figure 1. Auger spectra for a particular spot on the OFHC Cu plate. The lower panel shows the spectrum before sputter-cleaning; we noted peaks for C (250 eV), O (500 eV) and Cu. The upper panel shows the spectrum after sputter-cleaning for 3 min; the only peaks remaining are those for Cu (one at 50 eV, three between 750 eV and 1000 eV). Note scale change from lower to upper.

3.4. Dielectric function for amorphous materials at low temperatures

From the foregoing, we know the chemical composition and the approximate thickness of the surface film (for a surface which is properly prepared, so that we have no organic contamination or corrosion). We now wish to determine the dielectric dispersion of Cu_2O at low temperatures. Unfortunately, such a measurement has not been done. We instead argue as follows: amorphous materials have more low-temperature defect motion than crystalline materials. In addition, the low-T defect motion in amorphous materials tends to be quite similar for a broad range of chemistries/structures. Since the dispersion and loss at low temperatures is dependent on defect motion, we believe that it is reasonable to conclude that a conservative estimate of the dielectric dispersion and loss can be garnered by looking at experimental results in a variety of bulk amorphous materials.

Table 1 shows the low-T dispersion and/or loss for a variety of amorphous materials, at the noted frequency and temperature ranges.

What can we conclude from this long list? First of all, in the two cases where dispersion and loss were measured in the same material, the Kramers–Kronig relations are obeyed (i.e. the magnitudes are about the same). Secondly, in general, at temperatures below 1 K, it is clear that the dispersion and dissipation (in particular, $\delta\epsilon(f)/\epsilon$ and ϵ''/ϵ) are both less than 10^{-3}. Lastly, we can state that it is clear from the papers (not from just the table) that the dispersion and the loss do indeed fall strongly as the temperature falls.

Table 1. Literature survey of the dispersion ($\delta\epsilon(f)$) and dissipation (ϵ'') at low temperatures, for a wide range of amorphous materials.

Material	Reference	T	f	$\delta\epsilon(f)/\epsilon$	ϵ''/ϵ
Stycast 1266	[20]	0 K to 25 K	?	?	$< 10^{-6}$
polyethylene + dioct.	[21]	< 0.12	10 Hz to 10 kHz	?	$< 7 \times 10^{-4}$
BeF_2, GeO_2, SiO_2, As_2S_3	[22]	< 10 K	?	?	$< 2 \times 10^{-4}$
$(KNO_3)_{61}[Ca(NO_3)_2]_{39}$	[18]	< 20 K	?	?	about 10^{-3}
silicate glass, bioglass	[18]	< 20 K	?	?	$< 1.5 \times 10^{-3}$
BK 7 glass	[18]	9 mK to 4 K	10 Hz to 10 kHz	?	$< 10^{-3}$
PMMA	[18]	1.2 K to 4 K	0.01 Hz to 10^4 Hz	?	$< 10^{-4}$
P_2O_5 / 2% Nd_2O_3	[19]	10 mK to 1 K	1 kHz to 10 kHz	10^{-3}	$< 10^{-3}$
borosilicate glass		10 mK to 1 K	1 kHz to 10 kHz	10^{-3}	$< 10^{-3}$
poly-C_2D_4 + dibut. + 4-methyl ...	[23]	4 mK to 4.2 K	10 Hz to 10 kHz	?	$< 0.75 \times 10^{-3}$
amorph. $PbTiO_3$	[24]	< 0.1 K	1 kHz to 100 kHz	$< 7 \times 10^{-4}$	?
amorph. $PbTiO_3$	[24]	< 0.03 K	1 kHz to 100 kHz	$< 1 \times 10^{-4}$	?
cryst. $PbTiO_3$	[24]	< 0.1 K	1 kHz to 100 kHz	4×10^{-4}	?
cryst. $PbTiO_3$	[24]	< 0.05 K	1 kHz to 100 kHz	$< 1 \times 10^{-4}$	?
SiO_x	[25]	20 mK, 140 mK	500 Hz to 5 kHz	$< 0.5 \times 10^{-4}$	$< 10^{-4}$
mylar	[25]	20 mK, 140 mK	?	?	$< 10^{-4}$
K:SiO_2	[25]	2.5 mK, 140 mK	500 Hz to 5 kHz	$< 3 \times 10^{-6}$	?

3.5. Frequency dependence of dispersion

In order to use the foregoing to model the frequency dependence of $C_{\rm cryo}$ we need to know the dispersion $\delta\epsilon(f)$ over the frequency range of interest, from 0.01 Hz to 1 kHz. Table 1 has many results covering the higher frequency end of the range, but no results for the dispersion below 1 Hz. Although it appears likely from the table that the results at lower frequencies are similar, we can obtain an independent estimate by using the Kramers–Kronig relation. In particular, if we assume that the magnitude of the dissipation is constant as a function of frequency, then from equation (4) the change in the real part of the dielectric function from ω_a to ω_b is

$$\frac{\delta\epsilon(f)}{\epsilon} \approx \left(\frac{2}{\pi}\right)\frac{\epsilon''}{\epsilon}\ln\left(\frac{\omega_a}{\omega_b}\right). \tag{5}$$

If we set $\omega_a = 10^3$ Hz and $\omega_b = 0.01$ Hz, we thus obtain

$$\delta\epsilon(f)/\epsilon \approx 7\epsilon''/\epsilon \tag{6}$$

or

$$\delta\epsilon(f)/\epsilon \leqslant 7 \times 10^{-3}. \tag{7}$$

We note that this estimate is significantly larger than all the direct measurements of dispersion in table 1, and thus we are confident that this is a conservative estimate.

3.6. Numerical estimate of $\Delta C_{\rm cryo}(f)$

We note the following numerical quantities: (1) The capacitor plate separation for our design is $d = 0.05$ mm [16]; (2) the dielectric constant of Cu_2O is 9 [17]. Using equation (3), we finally obtain

$$\Delta C_{\rm cryo}(f)/C_{\rm cryo} \approx (10\,{\rm nm}/0.05\,{\rm mm})(1/9)(7 \times 10^{-3}) \approx 1.55 \times 10^{-7}. \tag{8}$$

We note that this estimate depends on the thickness of the surface films. Thus, in measurements of the ECCS, it is important to verify that the surfaces of the metal electrodes in the vacuum-gap capacitor have only the native oxide on them. Examples of failure would include organic contamination or corrosion of the metal surfaces. One simple way to ensure lack of organic contamination [15] would be to perform a sputter-clean with Ar^+ ions before quick assembly and then placement in the vacuum of the measurement cryostat.

4. Measurement of $\Delta C_{\rm cryo}(f)$ over a limited frequency range

As noted above, the crucial prediction of the model that we have derived is that the dispersion of the dielectric function falls off rapidly with temperature. As we noted in section 1, we cannot measure the dispersion over the entire frequency range nor at the low uncertainty that we aim to achieve. However, we have performed a measurement of $C_{\rm cryo}(f)$ over the range of frequencies from 100 Hz to 3 kHz; we have achieved an uncertainty of about $\delta C/C \approx 3 \times 10^{-7}$ at the bottom end of this frequency range and smaller uncertainties at higher frequencies.

We describe the sequence of measurements performed.

1. We measured the frequency dependence of a 10 pF standard, using our previously described technique [5].
2. We measured the frequency dependence of this same standard, using a commercial variable-frequency capacitance bridge. This allowed us to assess the frequency dependence of the bridge. In particular, the rated absolute uncertainty of the bridge at 100 Hz is about 10×10^{-6} relative to 10 pF; by calibrating using the standard, we were able to reduce the uncertainty by about a factor of 30.
3. We measured the frequency dependence of the cryogenic capacitor in vacuum as a function of time. When the value was stable enough (constant within desired uncertainty over the measurement time), we recorded a set of frequency-dependent measurements.

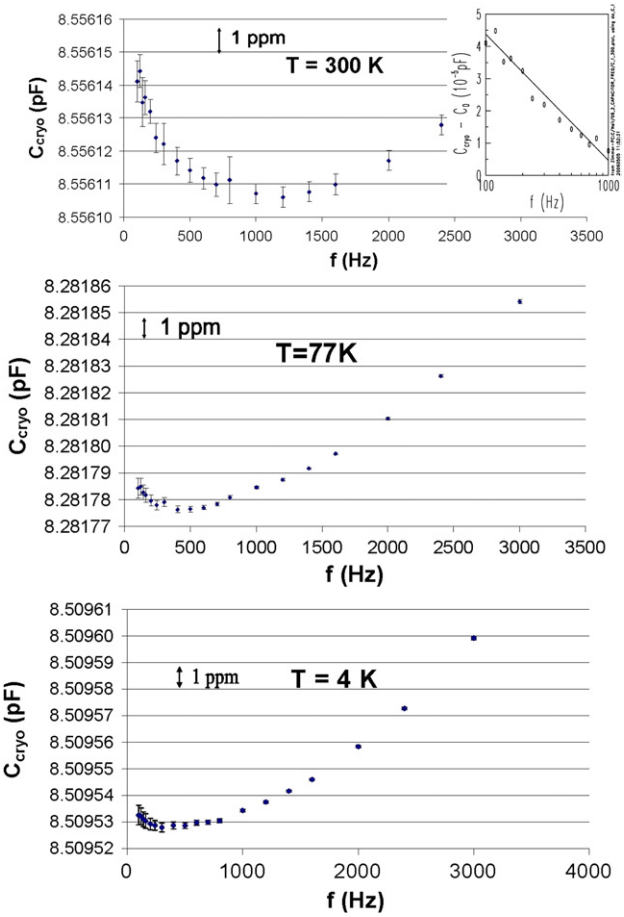

Figure 2. Capacitance measurements of the vacuum-gap capacitor at three different temperatures, as noted. The measurement has been adjusted for the frequency dependence of the bridge, as noted in the text. The uncertainties at the low frequency end are dominated by the uncertainty in the calibration of the frequency dependence of the bridge, due to the uncertainty in the measurement of the frequency dependence of the standard. The large increase in apparent value at higher frequencies is due to the cable loading, as determined by separate measurements. The major result of this figure is quite apparent: the low-frequency upturn in the capacitance at room temperature (due to dispersion) falls off rapidly at lower temperatures and is flat within the uncertainty at 4 K. In the inset of the upper panel, we show a semi-logarithmic plot for the data at 300 K; this plot confirms the prediction that the dispersion-induced frequency dependence should be logarithmic. $C_0 = 8.5561$ pF.

4. We then measured the standard again, to ensure that the frequency dependence of the bridge had not drifted.
5. We corrected the raw measurements of $C_{\rm cryo}$ using the results of the calibration with the standard. This correction was significant only at the low frequency end below 300 Hz, and its magnitude was less than 3×10^{-7} relative to 10 pF.

Figure 2 demonstrates manifestly the prediction of the model: the low-frequency dependence due to the dispersion in the surface films is very evident at room temperature. At lower temperatures, it falls off quite rapidly; $C_{\rm cryo}(f)$ is independent of frequency within the uncertainty of the measurement at 4 K (up to 1 kHz). We note that the prediction [11] for the low-frequency surface film-induced dispersion is a logarithmic dependence: $C_{\rm cryo} = a + b \ln f$. In the inset to the figure, we show a semi-logarithmic plot, confirming the prediction for our measurements.

We also note that there is a large frequency dependence at higher frequencies; we have verified that this is due to the cable loading by separate measurements. We can correct this high-frequency dependence, which is proportional to f^2, using the standard procedure mentioned above (not shown). After this adjustment, at 4 K $C_{\rm cryo}(f)$ is frequency-independent up to 1 kHz.

5. Conclusions

We aim to obtain the frequency dependence of $C_{\rm cryo}(f)$, in order to use the ECCS for capacitance calibrations and to close the quantum metrology triangle. Since we are unable to measure the frequency dependence, we have chosen to model the effect of surface films, which will dominate the low frequency behaviour. This model has one crucial prediction: $C_{\rm cryo}(f)$ gets much flatter as the temperature is decreased. This prediction is verified by measurements of $C_{\rm cryo}(f)$ over a limited frequency range, and it also allows us to conclude that there is very little frequency dependence of $C_{\rm cryo}(f)$ over the entire frequency range from 0.01 Hz to 1 kHz, at low temperatures.

We have made conservative assumptions throughout the derivation of this model, and therefore we are confident that its prediction is correct. In order to obtain a final result, we multiply our estimate by a small factor and thus conclude that the type B uncertainty in the ECCS due to the frequency dependence of the vacuum-gap capacitor is

$$\Delta C_{\rm cryo}(f)/C_{\rm cryo} = 2 \times 10^{-7}. \qquad (9)$$

Finally, we can comment on an additional usefulness of the cryogenic vacuum-gap capacitor which is made evident by the results of this work.

The frequency-dependent measurement of capacitance has recently been markedly extended by the introduction of a commercial variable-frequency capacitance bridge. It is evident that the process of measurements of capacitance standards has been and will continue to be strongly altered by the advent of this new bridge. However, as noted above, the absolute uncertainty of the measurement at the low-frequency end is about 10 ppm.

We suggest that, for practitioners in the field who may not wish to develop an ECCS, the cryogenic vacuum-gap capacitor by itself may provide a substantial advance: in combination with the commercial bridge, using the procedure outlined above to calibrate the frequency dependence of the bridge using $C_{\rm cryo}$, it may be possible in the future for such practitioners to deliver frequency-dependent measurements using the convenience of a commercial bridge but at a much lower uncertainty than that quoted for the bridge. As an example, we point out that in the field of low-temperature dynamics of amorphous materials, the broad range of activation energies or tunnelling times gives rise to the desire to measure capacitance over a wide range of frequencies; see for example [18, 19].

Acknowledgments

It is a pleasure to thank Scott Wight (NIST) for his advice and assistance with the surface measurements, Hansjoerg Scherer (PTB) for his encouragement and Art Hebard (U. Florida), Mark Keller and Dave Rudman (NIST) for useful discussions.

References

[1] Keller M W, Eichenberger A L, Martinis J M and Zimmerman N M 1999 A capacitance standard based on counting electrons *Science* **285** 1706
[2] Williams E R, Ghosh R N and Martinis J M 1992 Measuring the electron's charge and the fine-structure constant by counting electrons on a capacitor *J. Res. Natl Inst. Stand. Technol.* **97** 299–302
[3] Zimmerman N M and Keller M W 2003 Electrical metrology with single electrons *Meas. Sci. Technol.* **14** 1237–42
[4] Grabert H and Devoret M H 1992 *Single Charge Tunnelling* vol 294 (New York: Plenum)
[5] Wang Y C 2003 Frequency dependence of capacitance standards *Rev. Sci. Instrum.* **74** 4212–5
[6] Delahaye F and Goebel R 2005 Evaluation of the frequency dependence of the resistance and capacitance standards in the BIPM quadrature bridge *IEEE Trans. Instrum. Meas.* **54** 533–7
[7] Nakamura Y, Nakanishi M and Endo T 2001 Measurement of frequency dependence of standard capacitors based on the QHR in the range between 1 kHz and 1.592 kHz *IEEE Trans. Instrum. Meas.* **50** 290–3
[8] Small G W, Fiander J R and Coogan P C 2001 A bridge for the comparison of resistance with capacitance at frequencies from 200 Hz to 2 kHz *Metrologia* **38** 363–8
[9] Bego V, Butorac J and Gasljevic G 1989 Measurement of electrode surface effect in air capacitors using a precise coulombmeter *IEEE Trans. Instrum. Meas.* **38** 378–80
[10] So E and Shields J Q 1979 Losses in electrode surface films in gas dielectric capacitors *IEEE Trans. Instrum. Meas.* **IM-28** 279
[11] Inglis B D 1975 Frequency dependence of electrode surface effects in parallel-plate capacitors *IEEE Trans. Instrum. Meas.* **24** 133
[12] Zimmerman N M 1996 Capacitors with very low loss: cryogenic vacuum-gap capacitors *IEEE Trans. Instrum. Meas.* **45** 841
[13] Eichenberger A L, Keller M W, Martinis J M and Zimmerman N M 2000 Frequency dependence of a cryogenic capacitor measured using single electron tunnelling devices *J. Low Temp. Phys.* **118** 317–24
[14] Chawla S K *et al* 1992 An x-ray photo-electron spectroscopic investigation of the air-formed film on copper *Corros. Sci.* **33** 1617–31
[15] Matsuo P J *et al* 1999 Characterization of Al, Cu, and TiN surface cleaning following a low-K dielectric etch *J. Vac. Sci. Technol.* **17** 1435–47
[16] Zimmerman N M, El Sabbagh M A and Wang Y 2003 Larger value and SI measurement of the improved cryogenic capacitor for the ECCS *IEEE Trans. Instrum. Meas.* **52** 608–11
[17] Rakhshani A E 1991 The role of space-charge-limited-current conduction in evaluation of the electrical properties of thin Cu_2O films *J. Appl. Phys.* **69** 2365–7
[18] Gilchrist J Le G and Johari G P 1986 Low-temperature dielectric study of fused nitrates and other glasses *Phil. Mag.* B **54** 273–84
[19] Jinzaki Y, Okuda Y and Chan M H W 1984 Low temperature dielectric properties of phosphate glasses containing Nd_2O_3 *Japan. J. Appl. Phys.* **23** L106–8
[20] Barucci M *et al* 1999 Dielectric properties of Stycast 1266 over the 0.07–300 K temperature range *Cryogenics* **39** 963–6
[21] Gilchrist J 1996 Nonlinear dielectric properties of glasses at low temperatures *J. Mol. Liq.* **69** 253–67
[22] Phillips W A 1981 *Amorphous Solids 81* (Berlin: Springer)
[23] Gilchrist J and Godfrin H 1983 Secondary amines: a low-temperature dielectric relaxation study *Chem. Phys.* **79** 307–20
[24] Miura Y *et al* 1983 Dielectric constant of both amorphous and crystalline $PbTiO_3$ at low temperatures *J. Phys. Soc. Japan* **52** 1127–30
[25] Rogge S, Natelson D and Osheroff D D 1996 Evidence for the importance of interactions between active defects in glasses *Phys. Rev. Lett.* **76** 3136–9